Journal of Climate Change, Disaster Risk and Resilience Studies

Volume 1, Issue 1

Research Article

Date of Submission: 08 May, 2026
Date of Acceptance: 08 June, 2026
Date of Publication: 18 June, 2026

Multimodal Geophysical Characterization of Subsurface Structures - Insights from Independence Hall, KNUST, Ghana

Samuel B. Morfo[1], James Atsetso[1], Aggudey James[1], Mudigandla Rajesh[2], Bukari Ali[1] and Gurram Murali Krishna[2]*

[1]Department of Geological Engineering, Kwame Nkrumah University of Science and Technology, Kumasi, Ghana

[2]Department of Geo-Engineering, A.U. College of Engineering, Andhra University Visakhapatnam – 530003, India

***Corresponding Author:** Gurram Murali Krishna, Department of Geo-Engineering, A.U. College of Engineering, Andhra University Visakhapatnam, India.

Citation: Krishna, G. M., Morfo, S. B., Atsetso, J., James, A., Rajesh, M., et al. (2026). Multimodal Geophysical Characterization of Subsurface Structures - Insights from Independence Hall, KNUST, Ghana. *J Clim Change Disaster Risk Resil Stud, 1*(1), 01-09.

Abstract
A borehole drilling attempt at Independence Hall, KNUST, was unsuccessful due to an unexpected subsurface composition, a highly weathered and fractured layer beneath what was initially presumed to be the bedrock. To better understand the geological structure and recommend an optimal drilling approach, an integrated geophysical investigation was conducted. Seismic refraction, seismic reflection, and geo-electrical resistivity methods, including single-channel resistivity profiling and Electrical Resistivity Tomography (ERT), were utilized. A 200-meter survey line was established across the failed borehole site, with seismic refraction covering 100 meters, seismic reflection spanning 64 meters, and both ERT and single-channel resistivity surveys extending the full 200 meters. The results revealed a complex subsurface comprising three distinct layers including, a sandy topsoil, a sand and gravel formation, and a jointed-weathered granite layer. Seismic refraction data further indicated alternating competent and incompetent layers, with evidence of faulting. Despite the challenging subsurface conditions, the study suggests that the anomalous structure is not laterally extensive, and viable locations for drilling remain within the area. This investigation highlights the significance of geophysical surveys in delineating subsurface structures, optimizing borehole placement, and reducing the risk of drilling failures in geologically complex terrains.

Keywords: Seismic Refraction, Seismic Reflection, Geo-electrical Resistivity, Electrical Resistivity Tomography, Integrated Geophysical Methods, Fractured Bedrock, Borehole Failure

Introduction
A drilling attempt was made at a site within the Independence Hall of Kwame Nkrumah University of Science and Technology (KNUST) to establish a water supply borehole. However, the attempt was unsuccessful due to an unusual subsurface succession, characterized by a highly weathered and fractured layer underlying fresh rock, which was initially presumed to be the bedrock. This study integrates multiple geophysical methods, including single-channel resistivity profiling, seismic (refraction and reflection), and electrical resistivity tomography (ERT), to investigate the subsurface structure at the site. Several studies [1-9]. Have employed geophysical methods for subsurface characterization. Seismic refraction is widely applied in engineering and environmental research for determining parameters such as bedrock depth, water table depth, and lithological variations [10-14]. Additionally, seismic refraction techniques are particularly useful for identifying subsurface structural features, including faults and joints. The increasing need for engineering and environmental assessments has also led to the application of seismic reflection methods for investigating shallow subsurface targets relevant to hydrogeology, geotechnical engineering, archaeology and environmental studies [15-18]. The electrical resistivity method, primarily used from the early 1920s to the late 1980s as a one-dimensional (1D) imaging technique, was found to be insufficiently precise for complex geological settings [19]. Over the past two decades, advancements in multi-electrode arrays, automated acquisition systems, and inversion algorithms have significantly enhanced the capabilities of Electrical Resistivity Tomography (ERT), making it a versatile tool for detailed

subsurface investigations [20]. Vertical Electrical Sounding (VES) is traditionally employed to determine variations in resistivity with depth, particularly in horizontally stratified terrains with minimal lateral variation. However, to account for both vertical and horizontal resistivity variations, the Continuous Vertical Electrical Sounding (CVES) method is adopted. CVES integrates vertical electrical sounding with horizontal profiling, providing a more comprehensive subsurface image along a given profile.

Objectives

The primary objective of this study is to assess the subsurface structure at the Independence Hall, KNUST, with a focus on the sequence and competency of geological layers. Specifically, the study aims to determine the apparent resistivity distribution of the subsurface, evaluate the elastic properties and competency of the subsurface layers, and estimate their thickness. By achieving these objectives, the research seeks to provide valuable insights into the geotechnical characteristics of the site, which are essential for construction planning and infrastructural stability.

Justification

A previous attempt to drill a water supply borehole at the study site failed due to the unexpected presence of a highly weathered and fractured layer beneath what was assumed to be bedrock, leading to borehole collapse. To prevent similar failures, this study employs an integrated geophysical approach to comprehensively investigate the subsurface characteristics. Single-channel resistivity profiling and Electrical Resistivity Tomography (ERT) will map apparent resistivity variations, while seismic refraction and reflection surveys will assess the elastic properties, thickness, and competency of subsurface layers. The integration of these methods will help delineate the extent of the weathered layer, reconstruct the subsurface structure, and identify factors contributing to borehole instability. The findings will enhance geological understanding and support improved site selection for future drilling projects.

Study Area

The study site is located on the Kwame Nkrumah University of Science and Technology (KNUST) campus in Kumasi, Ghana, bounded by the coordinates (-1.57113, 6.6764), (-1.57115, 6.6783), (-1.57246, 6.6782), and (-1.57210, 6.6763), referenced to the World Geodetic System 1984 (WGS 84). Geologically, the area is underlain by basin-type granitoids, which are coarse-grained, plutonic, and associated with the Eburnean orogeny, a significant geological event that influenced the region's structural evolution. It falls within the Birimian meta-sedimentary terrain, consisting of phyllites, schists, greywackes, and slates [21]. These rock types influence groundwater potential, weathering profiles, and geotechnical properties. NUST is situated in the Oforikrom Municipality, within the wet sub-equatorial climatic region. The climate is warm and humid, with temperatures ranging from 21.5°C to 30.7°C and relative humidity levels averaging 84% in the morning and 60% in the afternoon. The area experiences a bimodal rainfall pattern, peaking in June and October, with an annual average of approximately 1,450 mm . Topographically, the terrain is predominantly low-lying and undulating, with a gentle west-to-east slope that influences drainage, soil erosion, and groundwater flow. Figure 1 presents a geological map of the Kumasi Metropolis, highlighting the stsudy location.

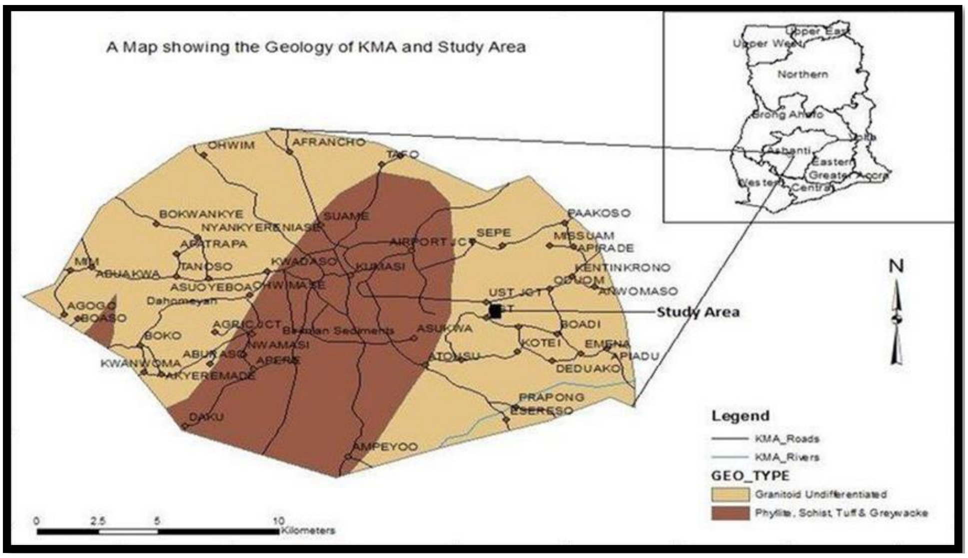

Figure 1: Geological Map of the Kumasi Metropolis (GSD, 2009)

Data And Methodology

A preliminary site investigation was conducted, comprising a desk study and a field reconnaissance survey. These assessments were essential for ensuring that the subsequent geophysical investigation would be effective and systematically executed. The desk study involved assessing and compiling previous field reports, geological maps, climate data, and vegetation characteristics of the study area. This step provided essential background knowledge regarding the presence of fractures, groundwater quality, depth to the water table, lithological sequences, climatic conditions, and vegetation cover. The reconnaissance survey aimed to analyze the physical characteristics of the site and establish an optimal traverse line for geophysical studies. This involved evaluating the geology and topography of the area, verifying the reliability of information obtained from the desk study, assessing social and logistical accessibility for field operations, and identifying the failed borehole point, where the traverse line was positioned for further investigation. The geophysical surveys conducted at the site included seismic refraction and reflection surveys, Electrical Resistivity Tomography (ERT), and single-channel resistivity profiling. These surveys were carried out along traverse lines of varying lengths, strategically positioned across the failed borehole site while considering methodological limitations and site constraints. A 100-meter traverse line was employed for the seismic refraction survey. The survey was conducted using a SmartSeis seismograph (Figure 2), eight geophones, a sledgehammer, and a metallic plate. The seismic refraction survey followed forward and reverse shooting techniques to ensure comprehensive subsurface coverage. The forward shooting procedure was conducted in three sets, based on geophone intervals and available equipment. The first three geophones were placed at 1 m, 3 m, and 5 m from the shot point to determine the crossover distance, preventing the omission of the first layer. The remaining geophones were spaced at 5-meter intervals to cover the entire 100 m traverse. The shot point was positioned at 0 m on the traverse line, ensuring seamless data acquisition and enabling deeper penetration. Seismic waves were generated using a sledgehammer and metallic plate, acting as the energy source. To enhance data quality, three stacking operations were performed at each shot point, increasing wave intensity and improving the signal-to-noise ratio. The procedure for reverse shooting mirrored that of forward shooting. The shot point was relocated to the 100 m position, with the 0 m point serving as the end of the traverse line. This ensured that subsurface data was captured symmetrically, improving interpretation accuracy.

Figure 2: The SmartSeis Seismograph for Seismic Refraction Survey

Seismic Reflection Survey

The seismic reflection survey was conducted using a SmartSeis seismograph, eight geophones, a sledgehammer, and a metallic plate. A measuring tape was laid along the traverse line, and shot points, as well as geophone locations, were marked accordingly. The total spread covered 64 meters, with geophones placed at 2-meter intervals. Shot points were positioned at 0, 8, 16, ..., and 48 meters along the traverse line. Seismic waves were generated by striking a metallic plate, which was pinned to the ground to improve ground contact, using a sledgehammer at each shot point. To enhance wave intensity and data reliability, three stacking operations were performed at each location. The resulting seismograms were recorded and stored using the seismograph. To optimize data acquisition, filters were applied to help the seismograph capture high-frequency signals of small amplitude, which might otherwise fall outside the dynamic range of the instrument. These filters also improved the signal-to-noise ratio, ensuring better resolution of subsurface features.

Electrical Resistivity Tomography Survey

Electrical Resistivity Tomography (ERT) measurements were conducted using an ABEM Terrameter LS, equipped with 81 stainless steel electrodes, electrical cables, sets of cable jumpers, a DC battery, and a hammer, as shown in Figure 3 and Figure 4. A single profile line of 200 meters in length was established, with electrodes spaced at 2.5-meter intervals.

Figure 3: ABEM Terrameter LS with Accessories

Figure 4: Mini-Res Resistivity Meter with Accessories

The Dipole-Dipole array was used for resistivity data acquisition due to its adequate depth of investigation and sensitivity to horizontal resistivity changes. During the apparent resistivity measurements, electrical cables were laid along a designated profile and linked to the ground using electrodes connected through cable jumpers at repeated take-out points. The ABEM Terrameter LS, powered by a battery, was used to measure apparent resistivity along the survey line. Data were recorded after ensuring all electrodes were properly connected. To maintain data quality, the contact resistances between electrode cables, take-out points, and cable jumpers were checked for faulty or failed electrodes. An electrode test was performed to verify the current flow through all planted electrodes. Contact resistance testing determined resistance to current flow due to surface conditions and loose connections. Measurements were automatically taken and stored in the Terrameter.

Single Channel Resistivity Profiling

The single-channel resistivity profiling was conducted using the Mini-Res resistivity meter and its accessories, including electrical cables and stainless-steel electrodes (Figure. 4). The survey was performed along a 200 m traverse line, with the failed borehole point at the center. Nine stations were investigated at 5 m intervals from Station 80 to 120 m, with the failed borehole at Station 100 m. The Schlumberger array was employed with a constant potential electrode separation of 8 m, and all stations were probed to a maximum depth (AB/2) of 80 m.

Data Processing

The seismic refraction and reflection survey data were processed using Pickwin software to determine the arrival times of refracted and reflected waves. The red ticks on the seismogram indicate the picked arrival times of waves from the same shot-point to various geophones. The arrival times identified in Pickwin were then transferred to Microsoft Excel® for further analysis. For the resistivity surveys, single-channel resistivity sounding data were also processed in MS Excel®. The recorded data from the ERT survey were downloaded from the ABEM Terrameter, and filtered to remove bad data points using MS Excel®.

Seismic Refraction

Figure 5 presents a seismogram from the first set of recordings on the traverse line. Distance-time graphs were plotted to identify the subsurface layers and calculate their seismic velocities using the inverse of the slopes (Equations 9 and 15). The corresponding layer thicknesses were determined using Equation 17.

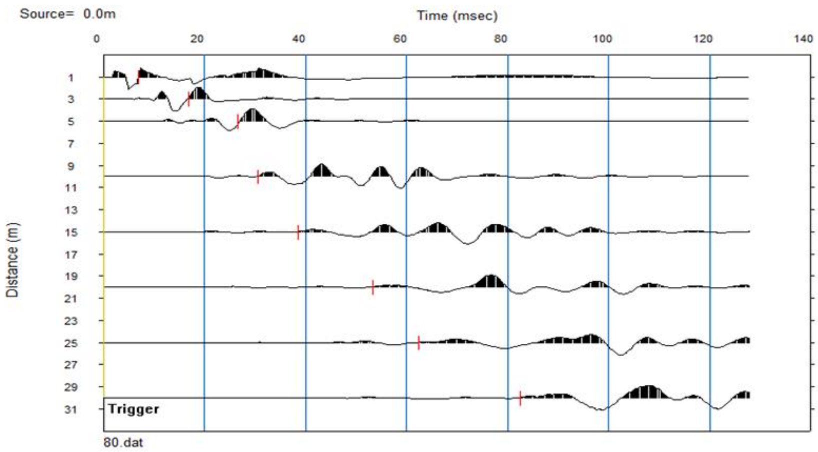

Figure 5: A seismogram Showing the Arrival Times of the Seismic Waves at the Geophones

Seismic Reflection

Figure 6 presents the arrival times of reflected waves from different subsurface layers. The seismogram displays the arrival times of waves from the first, second, and third layers. Red ticks on the seismogram indicate the picked arrival times of waves from the same shot point to various geophones, identified using Pickwin software. The offset distances (x) of the geophones and the corresponding arrival times (T) of the waves at the geophones were recorded. A graph of x^2 against T^2 was plotted, from which the seismic velocities of the various layers were determined using the inverse of the slopes (Equation 3). Additionally, the thicknesses of the layers were calculated using Equation 7.

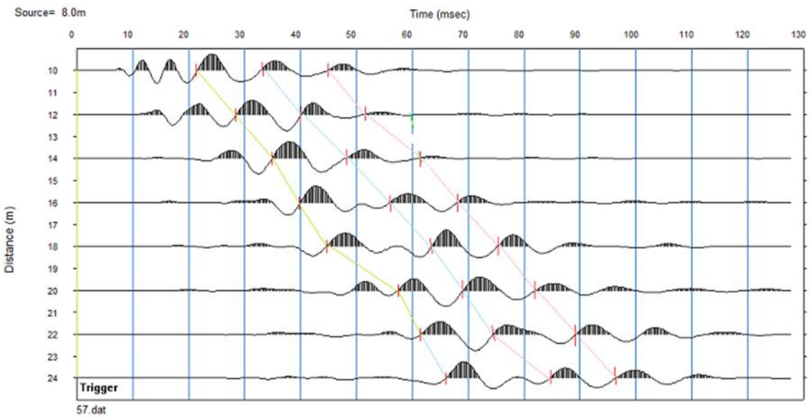

Figure 6: Seismogram Showing the Arrival Times Picked for Shot Point at 8 m

Electrical Resistivity Tomography

The recorded data from the ERT survey was downloaded from the ABEM Terrameter and processed using RES2DINV software to generate a 2D model of the subsurface resistivity distribution along the traverse line [22,23]. ERT measurements often contain outliers, such as negative resistivity readings or extremely high/low resistivity values, which can affect data quality. These bad data points, resulting from poor electrode ground contact (due to dry soil), relay failures, or shorting across cables in wet conditions, were identified and removed from the dataset. The L1 norm (robust) inversion technique was applied to refine the resistivity distribution by minimizing data misfit . The final 2D resistivity model was automatically generated in RES2DINV and saved as a Bitmap image format for interpretation.

Single Channel Profiling

Field measurements included resistance and electrode spacing at varying depths across different stations. The geometric factor was computed and used to derive apparent resistivities for each depth using Microsoft Excel. This processed data was then transferred to Surfer software to generate a 2D model of the apparent resistivity distribution of the subsurface.

Results And Discussion

Seismic Surveys

Figure 7 presents the distance-time graphs from the seismic refraction survey conducted at Independence Hall along a 100-m traverse line running North-South. The graphs reveal a highly complex subsurface, characterized by an intercalation of high- and low-velocity materials and the potential presence of near-vertical interfaces. Analysis of both forward and reverse shooting indicates the existence of five distinct subsurface layers. The summary of the seismic velocities for these apparent subsurface layers, obtained from the seismic refraction survey, is presented in Table 1.

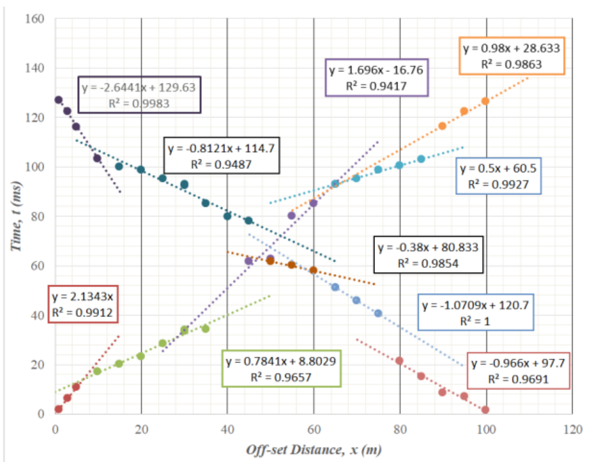

Figure 7: A distance-Time Graph for the Seismic Refraction Survey at Independence Hall

The seismic refraction survey conducted at Independence Hall, KNUST, revealed distinct subsurface layers with varying seismic velocities. From the forward shooting results, the first and third layers, with velocities of 468.54 m/s and 589.62 m/s, respectively, are interpreted as loose and dry soil, while the second layer, with a velocity of 1275.35 m/s, represents compact soil. The fourth and fifth layers, with velocities of 2000 m/s and 1020.41 m/s, respectively, suggest moderately weathered and highly weathered granitic rocks. In the reverse shooting, the first and second layers, exhibiting velocities between 933 and 1035 m/s, indicate coarse and compact soil. The third layer, with a velocity of 2631.58 m/s, is classified as slightly weathered granitic rock, whereas the fourth and fifth layers, with velocities of 1231.38 m/s and 378.20 m/s, respectively, are interpreted as weathered and jointed granitic rocks. Given that the study area is underlain by granitoids, the loose and dry soil layers are likely sandy, a common product of granite weathering, while the coarse and compact soil may be a sand and gravel formation derived from granitoids. The seismic velocity variations, as summarized in Table 1, further suggest an alternating sequence of competent and incompetent layers in the subsurface, highlighting its complexity and heterogeneity.

Layers	*Forward V_p (m/s)*	*Thickness (m)*	*Reverse V_p (m/s)*	*Thickness (m)*
1	468.54	2.21	1035.20	-
2	1275.35	-	933.79	9.90
3	589.62	14.77	2631.58	-
4	2000	7.31	1231.38	-
5	1020.41	-	378.20	-

Table 1: Summary Results of the Seismic Refraction Survey at Independence Hall, KNUST

In the forward shooting scenario, the orange and yellow lines exhibit near parallelism, as do the blue and grey lines (Figure. 8). Similarly, in the reverse shooting case, the light orange and light blue lines also appear nearly parallel. This alignment may indicate the existence of faults beneath the study area. Regarding the seismic reflection survey, five distinct subsurface layers can be identified (Figure. 8). Based on the velocity calculations presented in Table 2, the materials are likely to consist of loose and dry soil (UFC, 2008). The subsurface structure is highly complex, with certain layers absent at various points (Figure. 8). Specifically, the second layer from the surface is missing at stations 8, 17, and 32 meters, while the third layer is absent at stations 4, 6, 8, 16, and 48 meters. Furthermore, the fourth and fifth layers are missing at stations 8, 24, and 31 meters, as well as at stations 3, 8, 16, 24, 48, and 55 meters, respectively. Additionally, the boundaries between these subsurface layers are irregular and undulating.

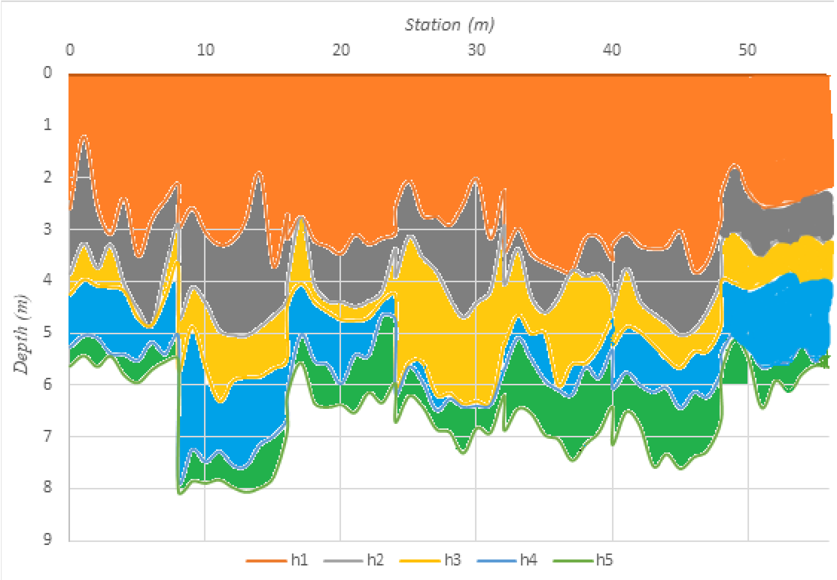

Figure 8: Subsurface Layering at Independence Hall, KNUST

Layers	1	2	3	4	5
V_p (m/s)	351	227	171	155	141

Table 2: Seismic Velocities for the Subsurface Layers Obtained from Seismic Reflection Survey

Electrical Resistivity Surveys

The Electrical Resistivity Tomography (ERT) image illustrating the subsurface resistivity distribution along the traverse line at Independence Hall is shown in Figure 9. The 2D inverted resistivity model represents the apparent resistivity values, ranging from 1.78 to 580.11 Ωm. The topmost layer exhibits resistivity values between 80 and 580 Ωm, extending up to a depth of approximately 11 meters and spanning from 0 to 200 meters along the traverse line. This layer is likely composed of dry sandy soil, possibly originating from the weathering of underlying granite rock. Directly beneath the surface layer, another formation is observed with apparent resistivity values ranging from approximately 30 to 120 Ωm. This formation extends laterally from station 35 to 175 meters along the traverse line and reaches depths of 11 to 34 meters. It is likely composed of sand and gravel, derived from highly weathered granite. Within this formation, several zones with significantly lower resistivity values (below 30 Ωm) are visible in blue, spanning the lateral positions 38–48 m, 65–80 m, 85–108 m, 147–155 m, and 165–173 m, at depths between 6 and 26 meters. These zones may indicate water saturation due to their relatively low resistivity. Additionally, another subsurface layer with apparent resistivity values ranging from 30 to 500 Ωm is identified at depths of approximately 34 to 49 meters, situated between stations 75 and 125 meters along the traverse line. This formation is likely a weathered granite, which may also contain water [24].

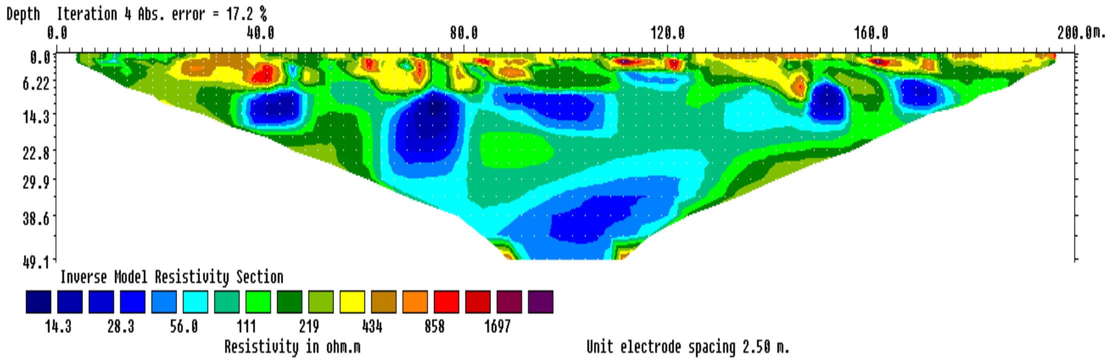

Figure 9: A 2D Resistivity Model Along the Traverse Line at the Independence Hall, KNUST

The 2D surfer model as illustrated in Figure 10 depicts the apparent resistivity distribution of the subsurface ranging from 17.26 to 461 Ωm.

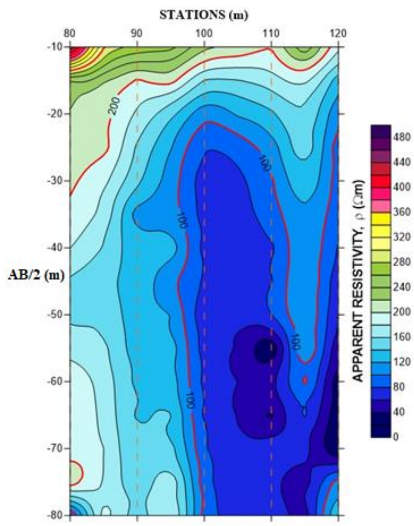

Figure 10: A 2D Surfer Model of Apparent Resistivity Distribution Along the Selected Traverse

The top layer, with apparent resistivity values ranging from 80 to 461 Ωm, extends laterally from stations 80 to 120 m and reaches a depth of approximately 30 m (AB/2). This layer is likely composed of dry sandy soil resulting from the complete weathering of the underlying granite bedrock. Between depths of 30 to 50 m (AB/2), the resistivity values range from 58 to 195 Ωm, suggesting the presence of sand and gravel. At greater depths (50 to 80 m AB/2), the 2D resistivity model indicates another formation with resistivity values between 30 and 214 Ωm, likely representing weathered, water-saturated granite, particularly between stations 105 to 110 m at depths of 52 to 68 m, where lower resistivity values are observed [24].

Conclusions

Integrated geophysical studies at Independence Hall, KNUST, revealed a three-layer subsurface structure consisting of dry sandy soil, a sand and gravel formation, and weathered granite. Seismic surveys indicated intercalated competent and incompetent layers, with a highly weathered, water-saturated zone between stations 95 and 115 m at depths of 37–44 m (ERT) and 52–68 m (single-channel resistivity profiling), likely causing borehole collapse. The thick low-resistivity zones suggest good groundwater potential. Drilling is recommended between stations 65–95 m and 115–130 m, while in the 95–115 m zone, it should not exceed 37 m to prevent collapse. A stronger seismic source is needed for deeper imaging, and direct boring should be conducted for unresolved structures [25].

Acknowledgements

We thank Almighty God for His guidance throughout this journey. Our deepest gratitude goes to our parents and our supervisor, Dr. Bukari Ali, for his invaluable support and encouragement. We also appreciate Prof. E.K. Appiah-Adjei, our Head of Department, for his unwavering guidance. Special thanks to the lecturers of the Geological Engineering Department for their support and to Mr. Bernard Ampofo for his technical advice.

Declarations

- **Clinical trial number:** not applicable.
- **Ethical Approval:** All ethical standards were adhered to during this study.
- **Data availability:** The datasets supporting the results of this study are included within the article.
- **Consent to participate:** Not applicable, as this research did not involve human participants or objects.
- **Consent to Publish:** All authors have read and approved the final manuscript and consent to its publication.
- **Conflict of Interest:** The authors declare no conflict of interest regarding this publication.

- **Funding:** Not applicable.

References

1. Nyako, S. O., Akyeampong, A. A., Ofosu, B., Opuni, K. O., & Mensah, F. A. (2017). Integrated geophysical methods for imaging the subsurface of a building site.
2. Bawuah, G., Baffoe, E., Darko, B., Hadir, I. A. A., & Ogbetuo, D. (2018). The use of seismic refraction survey in geotechnical investigations. International Journal of Engineering Research and Science, 4(7), 6-17.
3. Jacob, T., Samyn, K., Bitri, A., Quesnel, F., Dewez, T., Pannet, P., & Meire, B. (2018). Mapping sand and clay-filled depressions on a coastal chalk clifftop using gravity and seismic tomography refraction for landslide hazard assessment, in Normandy, France. Engineering Geology, 246, 262-276.
4. Pazzi, V., Morelli, S., & Fanti, R. (2019). A review of the advantages and limitations of geophysical investigations in landslide studies. International Journal of Geophysics, 2019(1), 2983087.
5. Shebl, S., Gemail, K. S., Attwa, M., Soliman, S. A., Azab, A., & Farag, M. H. (2019). Utilizing shallow seismic refraction in defining the geotechnical properties of the foundation materials: A case study at New Minia City, Nile Valley, Egypt. Egyptian Journal of Petroleum, 28(2), 145-154.
6. Mohammed, M. A., Abudeif, A. M., & Abd El-aal, A. K. (2020). Engineering geotechnical evaluation of soil for foundation purposes using shallow seismic refraction and MASW in 15th Mayo, Egypt. Journal of African Earth Sciences, 162, 103721.
7. Adewoyin, O. O., Joshua, E. O., Akinyemi, M. L., Omeje, M., & Adagunodo, T. A. (2021). Evaluation of geotechnical parameters of reclaimed land from near-surface seismic refraction method. Heliyon, 7(4).
8. Imani, P., Tian, G., Hadiloo, S., & Abd El-Raouf, A. (2021). Application of combined electrical resistivity tomography (ERT) and seismic refraction tomography (SRT) methods to investigate Xiaoshan District landslide site: Hangzhou, China. Journal of Applied Geophysics, 184, 104236.
9. Hasan, M., & Shang, Y. (2022). Geophysical evaluation of geological model uncertainty for infrastructure design and groundwater assessments. Engineering Geology, 299, 106560.
10. Calia, A., Leucci, G., Masini, N., Matera, L., Persico, R., & Sileo, M. (2012). Integrated prospecting in the crypt of the Basilica of Saint Nicholas in Bari, Italy. Journal of Geophysics and Engineering, 9(3), 271-281.
11. Andrews, N. D., Aning, A. A., Danuor, S. K., & Noye, R. M. (2013). Geophysical investigations at the proposed site of the KNUST teaching hospital building using the 2D and 3D resistivity imaging techniques.
12. Pegah, E., & Liu, H. (2016). Application of near-surface seismic refraction tomography and multichannel analysis of surface waves for geotechnical site characterizations: A case study. Engineering Geology, 208, 100-113.
13. Adelinet, M., Dominguez, C., Fortin, J., & Violette, S. (2018). Seismic-refraction field experiments on Galapagos Islands: A quantitative tool for hydrogeology. Journal of Applied Geophysics, 148, 139-151.
14. Alshehri, F., & Abdelrahman, K. (2021). Groundwater resources exploration of Harrat Khaybar area, northwest Saudi Arabia, using electrical resistivity tomography. Journal of King Saud University-Science, 33(5), 101468.
15. Griffiths, D. H. and King, R. F. (1981). Applied Geophysics for Geologists and Engineers. The Elements of Geophysical Prospecting. 2nd Edition. Pergamon Press, Great Britain.
16. Telford, W. M., Geldart, L. P., & Sheriff, R. E. (1990). Applied geophysics. Cambridge university press.
17. Sharma, P. V., (1997). Environmental and Engineering Geophysics, Cambridge University Press.

18. Kearey, P., Brooks, M., & Hill, I. (2002). An introduction to geophysical exploration (Vol. 4). John Wiley & Sons.
19. Keller, G. V., & Frischknecht, F. C. (1966). Electrical methods in geophysical prospecting.
20. Bing, Zhou (2018). Electrical Resistivity Tomography. A Subsurface-Imaging Technique, Applied Geophysics with Case Studies on Environmental, Exploration and Engineering Geophysics, Intech Open.
21. Kesse, G. O. (1985). The Mineral and Rock Resources of Ghana. AA Balkema Publishers, Netherlands. pp. 610.
22. Dahlin, T., & Loke, M. H. (1998). Resolution of 2D Wenner resistivity imaging as assessed by numerical modelling. Journal of applied geophysics, 38(4), 237-249.
23. Griffiths, D. H., & Barker, R. D. (1993). Two-dimensional resistivity imaging and modelling in areas of complex geology. Journal of applied Geophysics, 29(3-4), 211-226.
24. Reynolds, J. M. (2011). An introduction to applied and environmental geophysics. John Wiley & Sons.
25. Ghana Geological Survey, (2009). Geological map of Kumasi Metropolis.